ISSN 1560-8034, 1605-6582 (On-line), SPQEO, 2018. V. 21, N 3. P. 288-293

Optics

Electronic structure and optical properties of HgSe

J.O. Akinlami* **and O.O. Odeyemi**

Department of Physics, Federal University of Agriculture, P.M.B 2240, Abeokuta, Ogun State, Nigeria
**E-mail: johnsonak2000@yahoo.co.uk*

Abstract. We have performed the density functional theory calculations of mercury selenide compound using the plane-wave pseudo-potential (PWPP) method within the generalized gradient approximation to investigate the electronic structure and dielectric response of this compound in its zinc blende phase. The calculated lattice and volume parameters are in consonance with other experimental and theoretical works. The electronic structure of the compound showed that mercury selenide exhibited a semi-metallic property with a negligible direct band gap of about 0 eV at high symmetry gamma-point. Real and imaginary parts of dielectric function as a function of photon energy have been also obtained.

Keywords: density functional theory, structural properties, electronic structure, optical properties, mercury selenide.

doi: https://doi.org/10.15407/spqeo21.03.XXX
PACS 31.15.-p, 71.20.-b, 77.22.Ch, 78.20.Cl

Manuscript received 22.06.18; revised version received 31.08.18; accepted for publication 00.00.18; published online 00.00.18.

1. Introduction

Mercury selenide (HgSe) crystallizes in the zinc blende (ZB) structure at ambient temperature and pressure. It is characterized by high electron mobility, large electron concentration and variation of band gap with temperature [1]. The compound shows a large spectrum of properties making them good candidate for modern optoelectronics and spintronics due to its unique band structure [2, 3]. The Hg-VI system of selenium, tellurium and sulphur forms a group of compounds referred to as the mercury chalcogenides [2, 3], it is also useful in quantum electronics application [4]. Compared to other II-VI compounds, very few experimental and theoretical studies have been reported for the HgSe compound. Cardona *et al.* used *ab initio* calculation to investigate the electronic band structure and phonon dispersion relation of the ZB-type mercury chalcogenides [5]. Also, Delin and Kluner using the all-electron full-potential linear muffin-tin orbital method found that in zinc blende structure both HgSe and HgTe are semimetals [4]. Secuk *et al.* investigated the physical properties of HgTe and HgSe using ABINIT code within the local density approximation based on the density functional theory [6]. Arora and Ahujawe reported energy bands, density of states (DOS) and band gaps of these chalcogenides by using the Hartree–Fock and density functional theory [7]. El Haj Hassan *et al.* employed the full-potential linearized augmented plane wave (FP-LAPW) method within the density functional theory (DFT) in order to study the composition dependence of the lattice constant, bulk modulus and iconicity of HgSe, HgTe and their $HgSe_xTe_{1-x}$ alloys [8]. To the best of our knowledge, no experimental or theoretical calculation of HgSe by using plane-wave pseudo-potential (PWPP) method with GGA approximation has been performed. Based on this method, we have investigated the structural, electronic and optical (dielectric response) properties for this compound. All the calculations of the HgSe crystal involve two atoms per face-centered cubic unit cell. The computational methods are given in the section 2. The results and discussion are presented in the section 3, while the section 4 presents our conclusions.

2. Computational method

First-principle calculations were performed to study the structural, electronic and optical properties of HgSe by using the plane-wave pseudo-potential method within generalized gradient approximation. The structural and opto-electronic properties of mercury selenide were computed being based on the quantum mechanical modelling method. The calculations were performed using the ABINIT code (9) that implements the density functional theory by solving the Kohn–Sham [10] and Hohenberg and Kohn [11] equations describing electrons in a material, expanded in a plane-wave basis set and using a self-consistent conjugate gradient method to determine the energy minimum. Computational efficiency was achieved through the use of fast Fourier transforms [12] and pseudopotentials to describe core electrons. The electron exchange and correlation energies

were treated using the generalized gradient approximation (GGA) with Perdew–Burke–Ernzerhof (PBE) [13]. The pseudopotential of all atoms for the first-principle calculations was generated according to the scheme of Troullier and Martins [14] to generate norm conserving non-local pseudopotentials, which results in highly transferable and optimally smooth pseudopotential. The Brilloiun zone integration was replaced by discrete summations over a special set of *k*-points, by using the standard *k*-point technique of Monkhorst and Pack [15], where the *k*-point mesh used is 8×8×8 for the structural and electronics properties, while the large *k*-point of 24×24×24 was used for the optical properties in order to achieve a highly converged curves. The energy cut off to expand the wave function was set to be 680.3 eV. Plane waves were used as the basis set for the electronic wave functions. Basis functions were constructed by expanding around fixed energies. For the mercury atom, the 5*d* and 6*s* orbitals were considered as the valence orbitals, while for selenium, 4*s* and 4*p* electrons are the valence orbitals. Accurate convergence test were carried out with respect to the ground state energy.

3. Results and discussion

The results from the first principle calculations of the structural, electronic and optical properties of mercury selenide are grouped in Tables 1 to 3 and Figs 1 to 12.

Ground state properties

Plane-wave pseudo-potential based on density functional theory within generalized general approximations was used for the ground state properties calculations. The energy cut off and number of *k*-point are input parameters common to all the properties to be calculated. Figs 1a and 1b showed the graph of the total energy against the kinetic cut off and number of *k*-points, respectively. The kinetic cut off was optimized at 680.3 eV, while the number of *k*-point determined based on the Monk Horst Pack grid mesh was optimized at 8×8×8.

Table 1. Ground state (GS) properties of the equilibrium phase of HgSe.

Property	This work	Theoretical	Experimental
Lattice parameter (Å)	6.29	6.27 [8], 6.464 [17]	6.07 [16], 6.084 [18]
Bulk modulus (GPa)	44.79	44.70 [8], 40.21 [19], 41.80 [20]	57.60 [16]
GS volume ($Å^3$)	62.56	61.68 [5], 62.48 [6]	56.33 [16]

Table 2. Energy band gap of HgSe.

Property	This work	Theoretical	Experimental
Band gap (eV)	0.00	–0.55 [8], 0.00 [20]	–0.4 [16], –1.20 [18], 0.00 [5, 17], –0.1 [4]

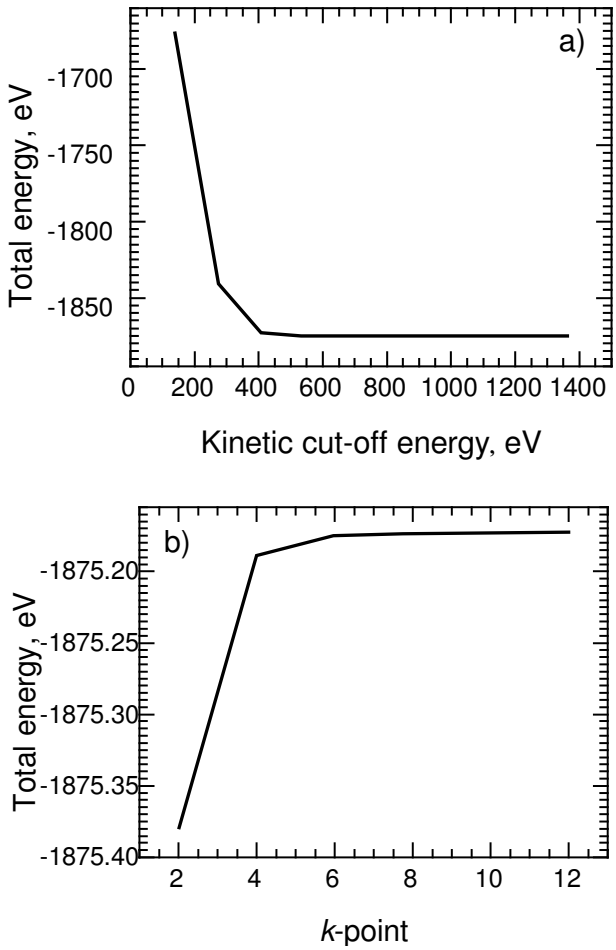

Fig. 1. Optimized kinetic energy cut-off (a); total energy *vs* number of *k*-point (b)

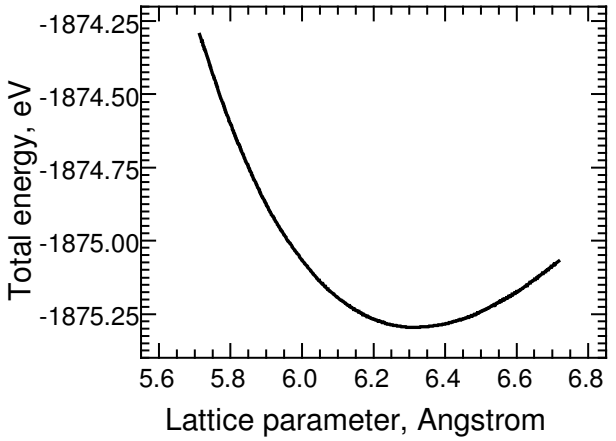

Fig. 2. Optimized lattice parameter of HgSe.

The plot of the total energy as a function of the lattice parameter is shown in Fig. 2. The calculation was made repeatedly for various values of the lattice parameters within 5.6 and 6.8 Å with an incremental value of 0.2 around the experimental value of 6.07 Å [16]. DFT was made within GGA, and it showed a typical overestimation, when being compared with the experimental value [11]. The plot of the total energy versus lattice parameter yields a parabola with a minimum at 6.29 Å. Our results are in good agreement

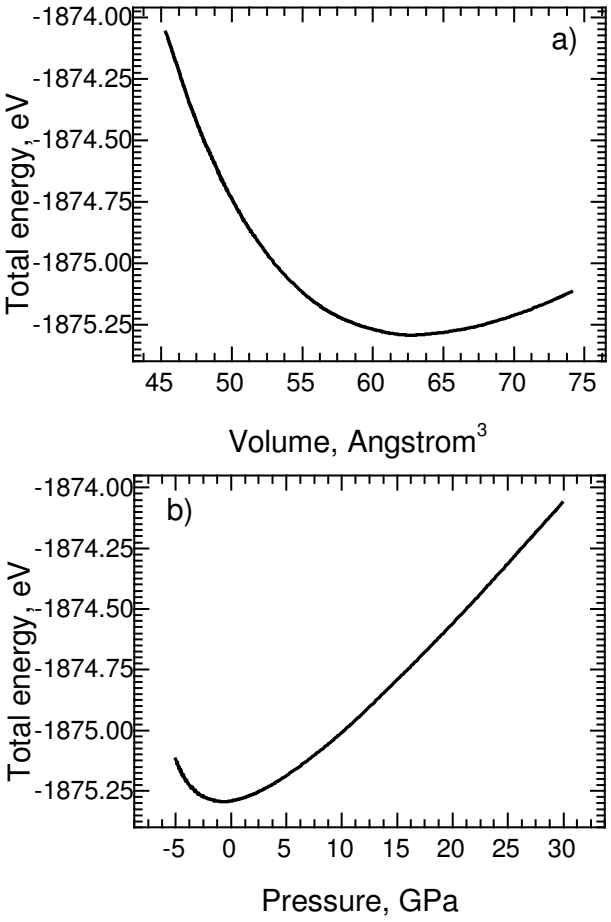

Fig. 3. Total energy *vs* volume (a) of HgSe, and total energy *vs* pressure (b) for HgSe.

with experimental and other theoretical values as shown in Table 1 and used for other calculations in this work. The curve of the total energy against the unit cell volume and that of the total energy against pressure is presented in Figs 3a and 3b, respectively. The total energy versus volume curve is a mirror of the total energy versus pressure curve. The volume parameter optimization was performed according to the total energy, and the volume parameter was obtained as 62.56 Å.

Electronic structure

The band structure was computed by solving the Kohn–Sham equation for many different *k*-points along the high symmetry wave path [9]. The electronic band structure of every compound is unique and useful to understand the electronic and optical properties of a material. As the atoms in solid state material are packed closer together with the interatomic separation distance to form a solid, their outer orbitals overlap and interact strongly with each other, and as a result electronic bands are formed [19]. The band structure shown in Fig. 4 was calculated with the energy optimized lattice parameter of 6.29 Å. The Fermi energy is automatically set at zero by the ABINIT code as indicated by the dotted horizontal line on the band structure plot. The electronic band structure of zinc blende HgSe at the calculated equilibrium lattice constant along the high symmetry *k*-path within the first Brillouin zone of its primitive cell is presented in Fig. 4. The calculation was performed within the energy range of –13 to +32 eV. As seen from the plot of the band structure calculation, HgSe crystal has a direct band gap at high symmetry gamma-point with a value of $5 \cdot 10^{-5}$ eV. This result agreed with previous work that mercury selenide is a zero gap semiconductor or a semi-metal [4]. This property makes it a good candidate for technological application in spintronics and optoelectronics. All features in the experimental band gap are observed in Fig. 4, and the overall electronic band profiles are in good agreement.

The calculated total density of state in Fig. 5 also shows a similar trend with the electronic band structure within the energy range –13 to 32 eV. DOS has several peaks, but the significant peaks were observed at –12.25, –6.39, –6.11, –4.66 and –2.30 eV. The total DOS result showed that the valence and conduction bands of HgSe are separated by a negligible band gap. The calculated density of states has its main peak of 38.67 states/eV at –6.12 eV with a shoulder peak of 28.69 states/eV at –6.49 eV.

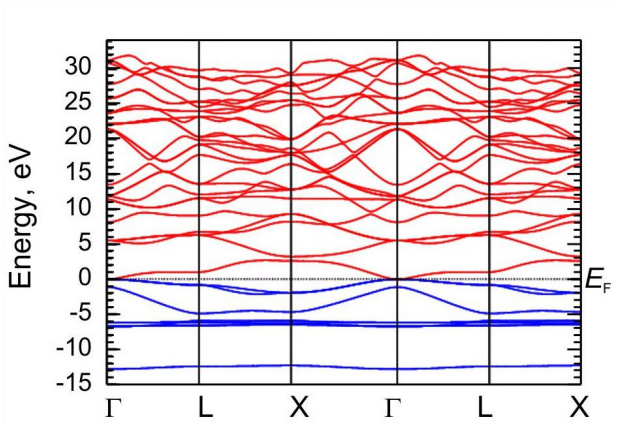

Fig. 4. Band structure of HgSe.

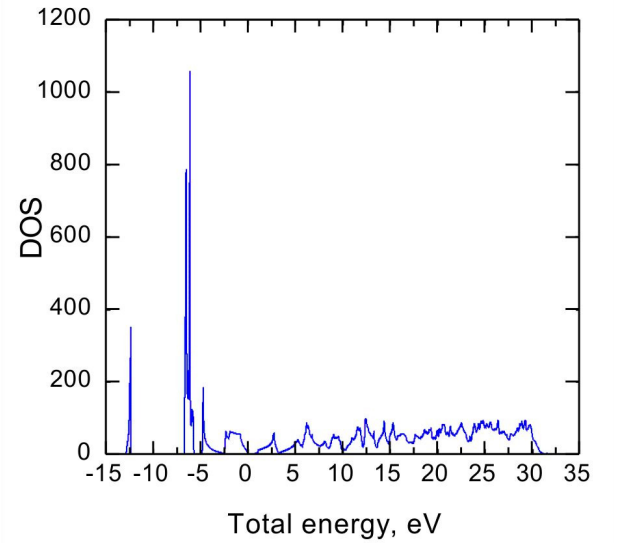

Fig. 5. Total density of states for HgSe.

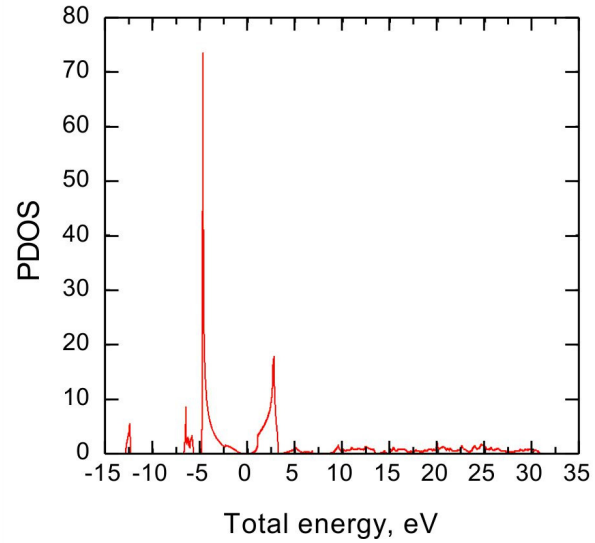

Fig. 6. PDOS for *s*-Hg valence orbital.

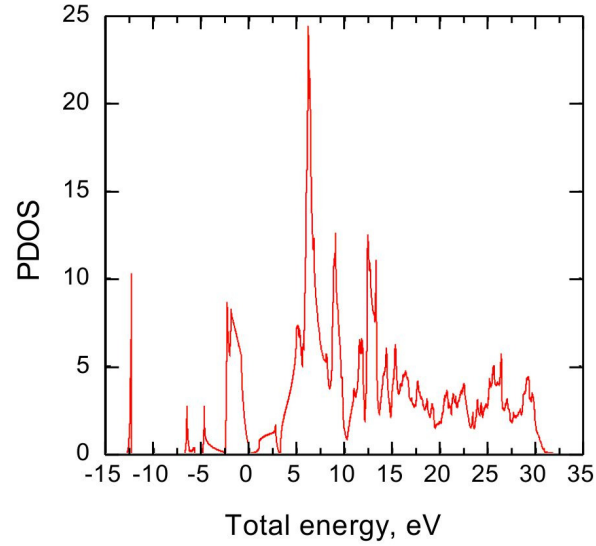

Fig. 7. PDOS for *p*-Hg valence orbital.

DOS in this compound showed three regions inside the valence band, the first is around –12.25, the second in the energy range of –6.76 eV and –5.66 eV, while the third is located around –4.93 and 0 eV. All the regions in the DOS curve correspond to the bands on the electronic band structure. There are several continuous bands in the conduction band with several minor peaks. The partial density of states (PDOS) plots showed the contribution of constituent orbitals to the total density of states. PDOS for the valence orbitals of the individual atom of mercury (*s*-Hg, *p*-Hg and *d*-Hg) and selenium (*s*-Se and *p*-Se) are presented in Figs 6 to 10. With the Fermi level set to zero, the region around –12.25 eV is dominated by 4*s*-states from Se atoms, and it matches with the lowest valence band in the calculated band structure of HgSe. The region around –6.76 to –5.66 eV is predominantly occupied by Hg 5*d*-states. This region is responsible for the maximum peak and the shoulder peak in the curve. The region between –4.93 to 0 eV contains atoms from

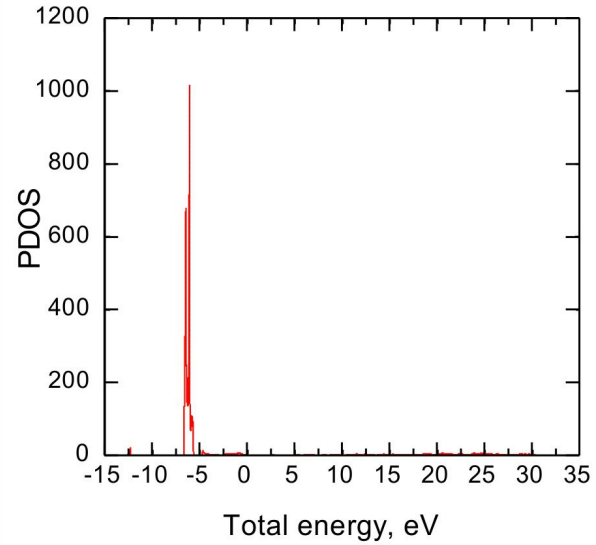

Fig. 8. PDOS for *d*-Hg valence orbital.

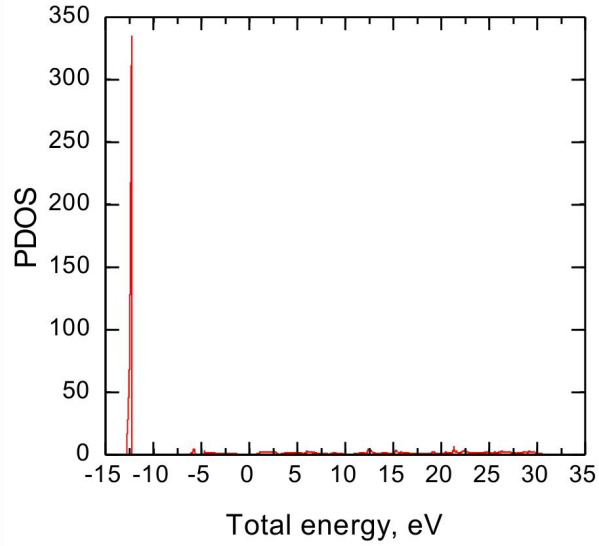

Fig. 9. PDOS for *s*-Se valence orbital.

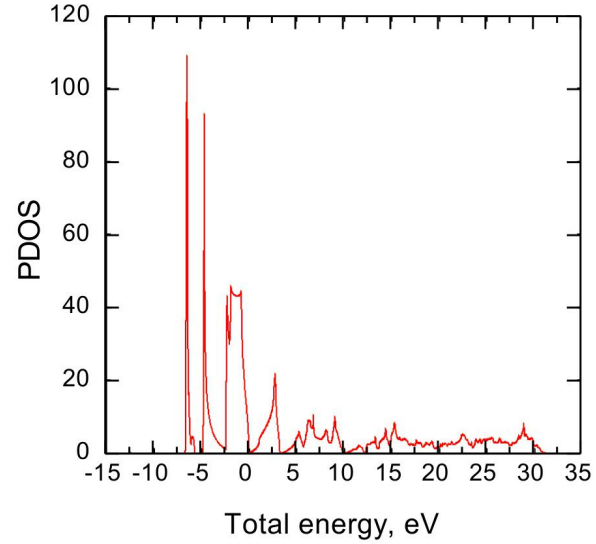

Fig. 10. PDOS for *p*-Se valence orbital.

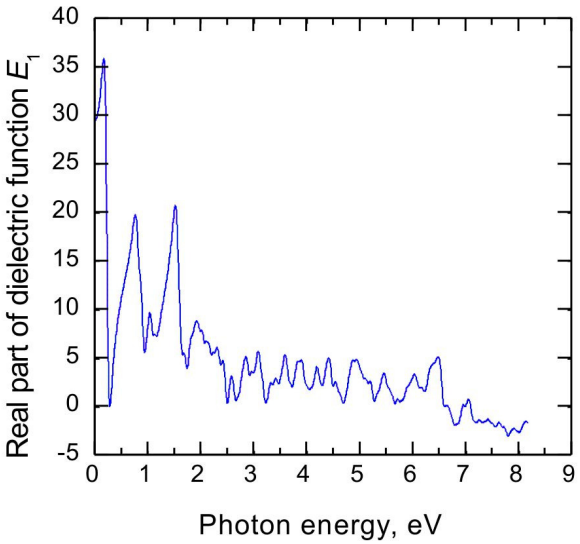

Fig. 11. Real part of dielectric function of HgSe.

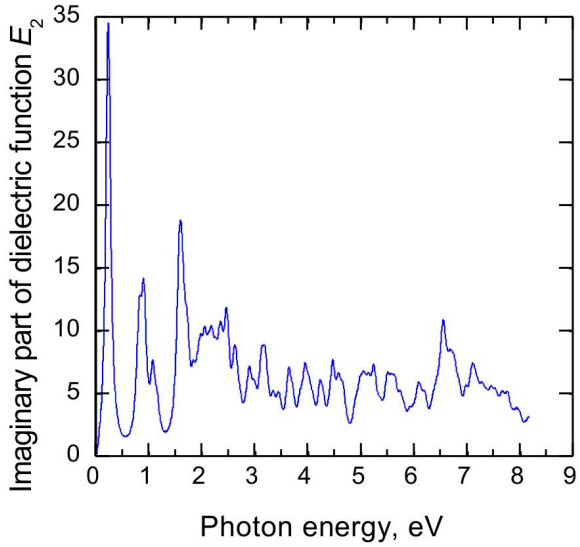

Fig. 12. Imaginary part of dielectric function of HgSe.

Table 3. The calculated static dielectric function ε_∞ of HgSe.

Property	This work	Theoretical	Experimental
Static dielectric function	29	13.5 [6]	26 [18]

Hg-6*s* and a minor contribution from Se-4*p* around the valence band maxima. These results correspond to the various valence orbital of mercury (5*d* and 6*s*) and selenium (4*s* and 4*p*).

Dielectric response

The optical properties can be obtained from the complex dielectric function that is usually connected with the electronic structure [19, 21]. HgSe crystal is an optic crystal, therefore the frequency dependent real and imaginary dielectric function of mercury selenide were calculated. The analysis of the overall spectrum provide important information about electronic band structure at *k*-points in the Brillouin zone, in particular at the points of high symmetry near the valence and conduction band edges. The *x*, *y* and *z* axes are indistinguishable in cubic crystals. Hence, zinc-blende HgSe has isotropic optical properties. The real (ε_1) and imaginary (ε_2) dielectric response was calculated within the energy range 0…8.2 eV. The real part of linear dielectric function, ε_1, goes to its maximum value 35.64 at the photon energy 0.18 eV for HgSe and drops immediately below zero to –0.0492 at 0.282 eV as shown in Fig. 11. Also, the curve goes to negative between the energy range 6.787 to 8.2 eV. At values below zero, the material acts as a metal, while it acts as a dielectric material above zero. Other peaks on the real part were at 0.18, 0.77, 1.06, 1.53 and 1.93 eV. The peaks on the real part of dielectric response are interpreted by direct interband transitions from the top of the valence bands to the lowest conduction bands. Also from Fig. 11, the static dielectric function is obtained as 29 and is compared with other experimental and theoretical works in Table 3.

The first peak, which is also the highest peak in the imaginary plot, started from zero and reached the peak value 34.52 for 0.244 eV photon energy. It then dropped to 14.10 at the photon energy 0.917 eV. Other peaks are located at 1.07 and 1.59 eV for HgSe. The peaks of the imaginary part of the dielectric function also correspond to optical transitions from the valence band to the conduction band. For HgSe, the absorption spectrum from the fundamental absorption edge at about 0 to 8.2 eV is interpreted by direct interband transitions from the top of the valence bands to the lowest conduction bands.

4. Conclusion

The first principle calculation of the structural, electronics and optical properties of mercury selenide was obtained using the plane-wave pseudo-potential method. DFT within GGA was used as the exchange correlation. The ground state properties including equilibrium lattice parameter, pressure and volume derivative and minimized total energy were determined. The results obtained agreed with other experimental and theoretical values. The energy band gap, total DOS, partial DOS were also determined in its zinc blende phase. The band gap of HgSe was found to be $5 \cdot 10^{-5}$ at high symmetry gamma-point within the energy range of –13 and +32 eV. The DOS and PDOS plot showed that the 5*d*- and 6*s*-orbitals for mercury and the 4*s* and 4*p* for mercury formed the valence band with the 5*d*-orbital of mercury responsible for the huge peak observed.

The real and imaginary parts of the dielectric function for the compound were also determined. HgSe crystal is an optic crystal, the compound has a static dielectric function value 29. The results obtained are in tandem with the known experimental and theoretical works. It is thus shown that mercury selenide in its zinc-blende phase exhibits a semi-metallic property at ambient temperature and pressure and has good application as optoelectronic materials.

References

1. Ren J., Eason D.B., Churchill L.E., Yu Z., Boney C., Cook J.W. Jr., Schetzina J.F., El-Masry N.A. Integrated heterostructure device composed of II–VI materials with Hg-based contact layers. *J. Cryst. Growth.* 1994. **138**, Issues 1-4. P. 455–463.
2. Gawlik K.U., Kipp L., Skibowski M., Orlowski N. and Manzke R. HgSe: Metal or Semiconductor? *Phys. Rev. Lett.* 1997. **78**. P. 3165–3168.
3. Chantis A.N, Schilfgaarde M.V. and Kutani T. Ab initio prediction of conduction band spin splitting in zinc blende semiconductors. *Phys. Rev. Lett.* 2006. 96. P. 086405 (2006). Erratum: *Phys. Rev. Lett*. 2006. **97**. P. 039903
4. Delin A., Klüner, T. Excitation spectra and ground-state properties from density-functional theory for the inverted band-structure systems β-HgS, HgSe, and HgTe. *Phys. Rev. B*. 2002. **66**, No 3. P. 035117.
5. Cardona M., Kremer R.K., Lauck R., Siegle G., Muñoz A., & Romero A.H. Electronic, vibrational, and thermodynamic properties of metacinnabar β-HgS, HgSe, and HgTe. *Phys. Rev. B*. 2009. **80**, No 19. P. 195204.
6. Secuk M.N., Aycibin M., Erdinc B., Gulebaglan S.E., Dogan E.K., Akkus H. Ab-initio calculations of structural, electronic, optical, dynamic and thermodynamic properties of HgTe and HgSe. *Amer. J. Condens. Matter Phys.* 2014. **4**, No 1. P. 13–19.
7. Arora G. and Ahuja B.L. Electronic structure of some mercury chalcogenides using Compton spectroscopy. *Radiation Physics and Chemistry*. 2008. **77**, No 1. P. 9–17.
8. El Haj Hassan F., Al Shafaay B., Meradji H., Ghemid S., Belkhir H., Korek M. Ab-initio study of the fundamental properties of HgSe, HgTe and their $HgSe_xTe_{1-x}$ alloys. *Physica Scripta*. 2011. **84**, No 6. P. 065601.
9. X. Gonze, Beuken J.-M., Caracas R. et al. First-principles computation of material properties: the ABINIT software project ABINIT. *Computational Materials Science*. 2002. 25, Issue 3. P. 478–492.
10. Kohn W. and Sham L.J. Self-consistent equations including exchange and correlation effects. *Phys. Rev*. 1965. **140**. P. A1133.
11. Hohenberg P. and Kohn W. Inhomogeneous electron gas. *Phys. Rev*. 1964. **136**. P. B864.
12. Goedecker S. Fast radix 2, 3, 4, and 5 kernels for fast Fourier transformations on computers with overlapping multiply-add instructions. Society for Industrial and Applied Mathematics. *J. Sci. Comput*. 1997. **18**, No 6. P. 1605–1611.
13. Perdew J.P., Bueke K., Ernzerhof M. Generalised gradient approximation made simple. *Phys. Rev. Lett*. 1996. **77**. P. 3865.
14. Martins J.L., Troullier N. Efficient pseudopotentials for plane-wave calculations. *Phys. Rev. B*. 1991. **43**. P. 8861.
15. Monkhorst H.J., Pack J.D. Special points for Brillouin-zone integrations. *Phys. Rev. B*. 1976. **13**, No 12. 5188.
16. Madelung O., Von der Osten W., Rossler U., in: Madelung O., Schulz M. Semiconductors – Basic Data. Springer, 1987; Landolt-Börnstein: Numerical Data and Functional Relationships in Science and Technology, in: New Series, Group III, Vol. 22, Springer Verlag, Berlin.
17. Boutaiba F., Zaoui A. and Ferhat M. Fundamental and transport properties of ZnX, CdX and HgX (X = S, Se, Te) compounds. *Superlattices and Microstructures*. 2009. **46**. P. 823–832.
18. Adachi S. *Handbook on Physical Properties of Semiconductor*. Berlin: Springer. 2004. Vol. 3.
19. Fox M., *Optical Properties of Solids*. Second edition. Oxford University Press, Oxford. 2010.
20. Wang X., Dou S. Xue. and Zhang C. Zero-gap materials for future spintronics, electronics and optics. *NPG Asia Materials*. 2010. **2**, No 1. P. 31–38.
21. Philipp H.R. and Ehrenreich H. Optical properties of semiconductors. *Phys. Rev*. 1993. **129**. P. 1550–1560.

Authors and CV

AKINLAMI, Johnson Oluwafemi, born in 1972, defended his Doctoral Dissertation in Physics (Theoretical Condensed Matter Physics) in 2011. **Senior Lecturer** at Federal University of Agriculture, Abeokuta, Ogun State, Nigeria. Authored over 20 publications. The area of his scientific interests includes optical properties of A^3B^5 and A^2B^6 compounds, photoemission study of the electronic structure of A^2B^6 compounds and layered oxysulfide (LaO)CuS, magneto-optical properties of solids.
Department of Physics, Federal University of Agriculture
E-mail: johnsonak2000@yahoo.co.uk

ODEYEMI, Oluwaseun Oladipupo, born in 1979, MSc in Physics (Condensed Matter Physics) in 2017. Assistant Chief Technical Officer Federal Radio Corporation of Nigeria (Paramount FM Abeokuta Ogun State). The area of his scientific interests includes first-principle calculations in electronics, structural, optical properties and applications of A^2B^6 compounds.
Department of Physics, Federal University of Agriculture